Biomaterials Science

ROYAL SOCIETY OF CHEMISTRY

PAPER

View Article Online
View Journal | View Issue

Cite this: *Biomater. Sci.*, 2023, **11**, 3144

Fe and C additions decrease the dissolution rate of silicon nitride coatings and are compatible with microglial viability in 3D collagen hydrogels†

Estefanía Echeverri, ‡[a] Charlotte Skjöldebrand, ‡[a] Paul O'Callaghan, [b] Anders Palmquist,[c] Johan Kreuger, [b] Gry Hulsart-Billström[d] and Cecilia Persson *[a]

Silicon nitride (SiN) coatings may reduce unwanted release of metal ions from metallic implants. However, as SiN slowly dissolves in aqueous solutions, additives that reduce this dissolution rate would likely increase the lifetime and functionality of implants. Adding iron (Fe) and carbon (C) permits tuning of the SiN coatings' mechanical properties, but their effect on SiN dissolution rates, and their capacity to reduce metal ion release from metallic implant substrates, have yet to be investigated. Such coatings have recently been proposed for use in spinal implants; therefore, it is relevant to assess their impact on the viability of cells expected at the implant site, such as microglia, the resident macrophages of the central nervous system (CNS). To study the effects of Fe and C on the dissolution rate of SiN coatings, compositional gradients of Si, Fe and C in combination with N were generated by physical vapor deposition onto CoCrMo discs. Differences in composition did not affect the surface roughness or the release of Si, Fe or Co ions (the latter from the CoCrMo substrate). Adding Fe and C reduced ion release compared to a SiN reference coating, which was attributed to altered reactivity due to an increase in the fraction of stabilizing Si–C or Fe–C bonds. Extracts from the SiN coatings containing Fe and C were compatible with microglial viability in 2D cultures and 3D collagen hydrogels, to a similar degree as CoCrMo and SiN coated CoCrMo reference extracts. As Fe and C reduced the dissolution rate of SiN-coatings and did not compromise microglial viability, the capacity of these additives to extend the lifetime and functionality of SiN-coated metallic implants warrants further investigation.

Received 16th December 2022,
Accepted 7th March 2023

DOI: 10.1039/d2bm02074b

rsc.li/biomaterials-science

Introduction

The release of metal ions and debris from metallic implants in the body can give rise to a localized adverse reaction to metal debris (ARMD).[1] These reactions include metallosis (metal poisoning) and aseptic lymphocytic vasculitis associated lesions (ALVAL), which can limit the implant's lifetime.[2–5] These conditions have been studied for metal-on-metal joint replacements, but it has also been observed in other metallic implants, such as spinal instrumentation,[3] which is of particular concern due to their proximity to the spinal cord and spinal nerves. Although spinal implants are not in direct contact with the central nervous system, metallic wear particles may diffuse into tissues surrounding the implant site. For example, such particles can disrupt the structural integrity of the meninges leading to adverse effects.[6–8] A specific mechanism of metallosis has not been identified, but likely involves a hypersensitivity reaction that results in inflammation and pain. Such symptoms could require revision surgeries and substantially reduce the patient's quality of life.[9,10]

In efforts to reduce the generation of wear particles and the release of ions, metallic knee implants have been covered with ceramic coatings.[11–14] SiN has been proposed as an alternative coating material due to its capacity to reduce wear and ion release from metallic substrates, while also possessing bacteriostatic properties.[15–18] SiN undergoes hydrolysis when exposed to aqueous environments, leading to its slow dissolution, which releases biocompatible ions.[19–26] The solubi-

[a]*Division of Biomedical Engineering, Department of Materials Science and Engineering, Uppsala University, Sweden. E-mail: cecilia.persson@angstrom.uu.se*
[b]*Department of Medical Cell Biology, Science for Life Laboratory, Uppsala University, Sweden*
[c]*Department of Biomaterials, University of Gothenburg, Sweden*
[d]*Translational PET Imaging, Department of Medicinal Chemistry, Uppsala University, Sweden*

†Electronic supplementary information (ESI) available. See DOI: https://doi.org/10.1039/d2bm02074b

‡These authors contributed equally.

lity of any wear particles into biocompatible ions may indeed reduce the risk of adverse immune responses. On the other hand, a too high dissolution rate limits the life time of the coating. Therefore, it is relevant to investigate possibilities of decreasing the coatings' dissolution rate, while maintaining their biocompatibility.

The dissolution rate of SiN coatings may be optimised by alloying with Cr and Nb;[27] however, concerns remain regarding the biocompatibility of these elements.[28] Alloying with biocompatible elements such as Fe and C could also alter the dissolution rate, and SiN coatings alloyed with C result in Si bonding to C, which alters the binding energy.[29–31] Fe has similar potential while being biocompatible.[32–35] In a previous study,[36] we found that addition of Fe reduced the hardness and elastic modulus of the coating, while not affecting the surface roughness or coating morphology. This is potentially beneficial for adhesion of the coating to the metallic substrate. In addition, the coatings were compatible with pre-osteoblastic cells (MC3T3) viability in a direct contact *in vitro* test. However, as those coatings were deposited on Si wafers, their ability to reduce metal ion release from a metallic substrate was not investigated, nor was their effect on dissolution behaviour. Furthermore, as these coatings have been considered for use in spinal implants, their effect on cell-types in close proximity to the implant site are of great interest. Here microglia cells were chosen as they are the resident macrophages (immune cells) of the CNS and represent the first line of defense against pathogens and other toxic insults. While the traditional manner of studying cell responses *in vitro* in 2D monolayer cultures can provide valuable information, key characteristics of the physiological environment are not readily recapitulated.[37] 3D culture models, in which cells are cultured in hydrogels, better reproduce their spatial arrangement and provides extracellular matrix interaction sites. This permits investigation of cellular responses in more complex environments, which may better model the *in vivo* situation. Therefore, this study aimed to investigate the dissolution behaviour of SiN coatings with Fe and C as additives, and the viability of microglia exposed to their liquid extracts in 2D and 3D culture models.

Materials and methods

Coating deposition

Coatings of Si, N, Fe and C were deposited onto Si wafers (University Wafer Inc, MA, United States) and on a metallic relevant substrate, cobalt chromium molybdenum discs (CoCrMo, Peter Brehm GmbH, Germany), using a physical vapour deposition technique built in house.[38] The source material of Si, Fe and C were in the form of solid targets with a purity of 99.99% (ScoTech, Scotland, United Kingdom), while N was introduced as a reactive gas alongside the sputtering argon gas. Prior to deposition the chamber had a base pressure of 10^{-9} Torr and during deposition the gases were supplied at a flow of 10.00 sccm and 3.00 sccm, for Ar and N respectively, to achieve a deposition pressure of 3×10^{-9} Torr. The Si, Fe and C targets were positioned at an angle of 45° to the substrate normal direction in order to achieve compositional gradients.[36] The substrates, nine CoCrMo discs, were placed in a 3 × 3 grid (Fig. 1a). This resulted in the intended gradients, where each sample had a different chemical composition. The deposition on individual discs enabled further characterization according to the study aims. The SiN reference coatings were deposited using the same parameters without the Fe and C targets.

Material characterization

The composition was obtained by X-ray photoelectron spectroscopy (XPS, Quantera II, Physical Electronics, USA) using a monochromatic Al-Kα source. Measurements were taken at the surface, after 3 min of sputtering at 200 V, and after an additional 15 minutes of sputtering at 200 V with Ar^+ ions. Core level spectra were evaluated after Shirley type background corrections with the software CasaXPS.

The surface roughness was evaluated by vertical scanning interferometry (VSI, NexView, ZYGO, Berwin, PA, USA) in 5 spots on the sample using 10× objective and 1× zoom.

In addition, the surface was imaged by scanning electron microscopy (SEM, Merlin, Zeiss, Germany) at a voltage of 1 kV and a current of 80 pA. The thickness of the coating was evaluated by assessing focused ion beam (FIB) cross-sections in the

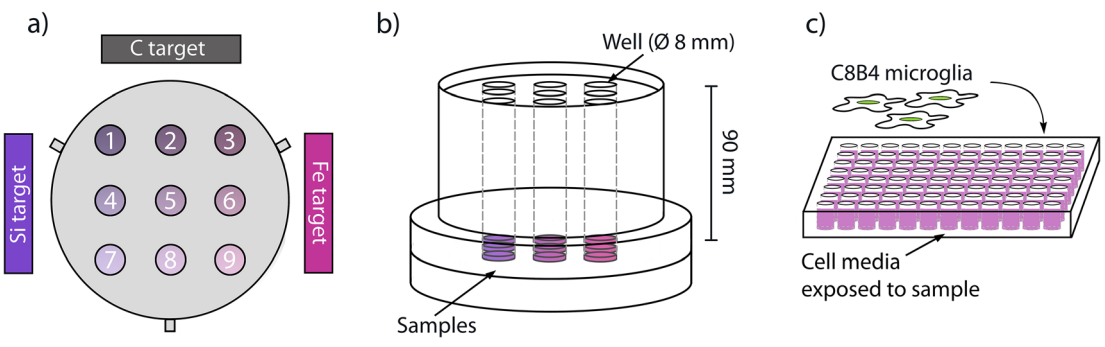

Fig. 1 A schematic illustration (a) of the sample placement in relation to the targets during deposition and the 9 resulting samples. The samples were mounted in a set-up (b) with wells that were filled with medium and 1% penicillin streptomycin, which allowed for isolated spots to be exposed to the liquid. After 14 days the leach was used to evaluate ion release. (c) Cytotoxicity was evaluated in a 2D cell culture assay with microglia (C8-B4) cells exposed to sample extracts from the various coatings.

SEM (FEI Versa 3D dual beam, FEI Company, Eindhoven, Netherlands). A thin layer of platinum was deposited over the site of interest to avoid any potential damage to the coating from the ion beam. Trenches around the site were milled using Ga^+ ions at 30 kV for rough milling (5000 nA) and polishing (300 nA). The samples were analyzed with an Everhart–Thornley detector at an acceleration voltage of 5 kV and current of 8 nA. Five regions of interest were evaluated per sample before and after the dissolution test.

Dissolution tests

The coatings were exposed to a solution of DMEM cell media and 1% penicillin streptomycin in a custom-made device (Fig. 1b).[27] The device allowed for isolating spots with an area of 78.5 mm^3 (cylindrical wells with 8 mm diameter) on the sample to be exposed to the solution. To avoid potential contamination, FBS was not added to the solution during the exposure phase. In addition, prior to incubation with the cell media the device was autoclaved and the sample sterilized by immersion in 70% isopropanol for 10 minutes. The wells were then filled with 4 ml of solution (surface area to extraction volume ratio 0.47 cm^2 mL^{-1}) and incubated at 37 °C and 5% CO_2 for 14 days.

After 14 days the solution was collected and investigated in inductively coupled plasma optical emission spectrometry (ICP-OES PekinElmer, Avio 200) to measure the concentration of released Fe, Co and Si ions. To avoid Si contamination from glassware extract handling was done with plastic utensils.

Afterwards, the samples were rinsed under deionized water followed by sonication for 10 min in deionized water, 10 min in 0.02% (v/v) detergent and 10 min in 70% (v/v) ethanol. In between each sonication the samples were rinsed in deionized water and finally the samples were dried using pressurized air.

Indirect cytotoxicity tests

Our previous study with SiFeCN coatings gave positive indications of biocompatibility using pre-osteoblastic cells[36] and subsequently the *in vitro* study on the microglial cells was proceeded to.

Mouse microglia cells C8-B4 (ATCC® CRL-2540) were cultured in Dulbecco modified Eagle's medium (DMEM) (ATCC 30-2002) supplemented with 10% fetal bovine serum (FBS, Gibco™ 26140079) and 1% penicillin/streptomycin (Sigma-Aldrich P433), incubated at 37 °C and 5% CO_2 and passaged upon reaching 70% confluency every 7 days.

Cytotoxicity of the SiFeCN coated samples, a reference SiN coating and CoCrMo controls was evaluated by testing leach extracts from the dissolution tests using the tetrazolium dye MTT, which reports on cell viability as a product of metabolic activity. C8-B4 cells were seeded in 96 well plates at a cell density of 10 000 cells per well and incubated for 24 hours, after which the media was replaced with extracts. Samples were evaluated in triplicates. The obtained extracts were diluted (1 : 32, 1 : 48, 1 : 64 and 1 : 80) and the cell viability was assessed on days 1, 2 and 3 after the cells were exposed to the extracts. Culture media served as untreated control, and 50% DMSO served as positive control. The absorbance of each extract was normalized to the untreated control. Data are presented as the mean ± standard deviation of at least three independent experimental replicates. Extracts presenting viability below 70% were considered cytotoxic.[39]

A 3-dimensional culture was also prepared, where C8-B4 cells were seeded at 2×10^6 cells per ml into collagen gels. The collagen gels were prepared by adding 17% v/v cell suspension in supplemented DMEM, 33% v/v collagen (rat tail type 1 collagen, Gibco, 3 mg ml^{-1} – A10483-01) and 50% v/v sup-

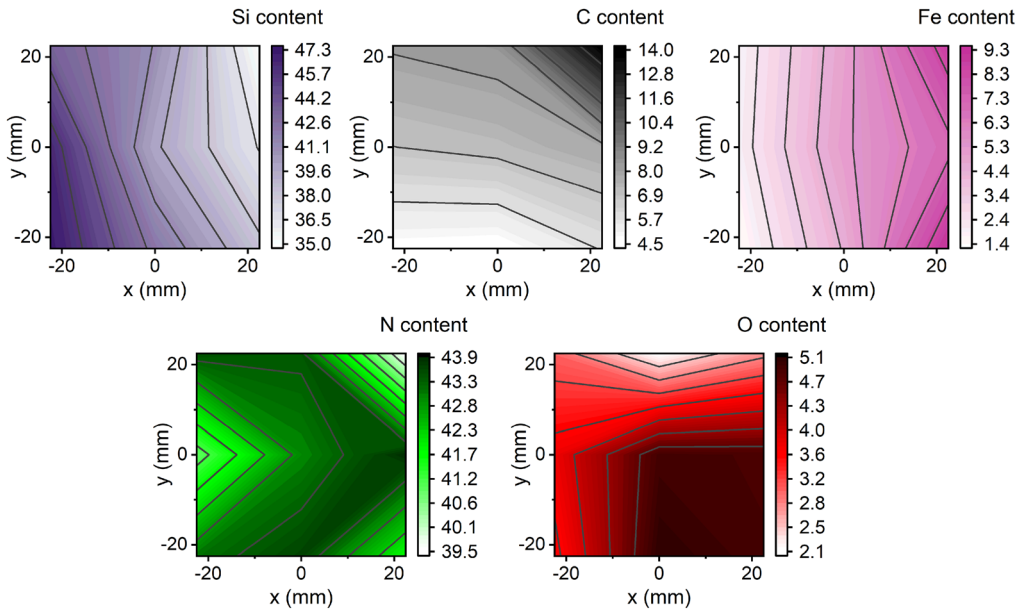

Fig. 2 The composition in at% obtained with XPS; the Si, C and Fe gradients are as expected based on the target placement during deposition, while N and O did not exhibit any trends.

plemented DMEM on ice. The reagents were gently mixed to evenly distribute cells throughout the gel, and the acidified collagen was neutralised using sodium hydroxide, confirmed by the yellow to pink colour change of the phenol red indicator in the DMEM media. 50 μL collagen gels containing cells were seeded into 18-well chamber coverslips (IBIDI μ-Slide 18 well – 81817) and incubated for 20 minutes at 37 °C and 5% CO_2 to permit collagen polymerization. Subsequently 80 μL of supplemented (10% FBS) DMEM were added to each gel, which were incubated in a cell culture incubator for 24 hours. Thereafter, the media was replaced with extracts diluted 1 : 64 (n = 3). 80% DMSO served as positive control. Cell viability was assessed after 1 and 3 days using a live/dead cytotoxicity kit for mammalian cells (Invitrogen™ L3224), which consists of green-fluorescent calcein-AM to detect intracellular esterase activity and red-fluorescent ethidium homodimer (EthD), which binds to DNA in cells with impaired plasma membrane integrity. Live/dead stained microglia in hydrogels exposed for 1 and 3 days were imaged at 3 locations using confocal laser scanning microscopy (CLSM) (Leica, SP8) using the 10× objective lens to take Z-stacks images with an optical section thickness of 4.2 μm, to produce a total of 36 stacks. Living cells are presented in green and dead cells in magenta.

Image analysis of live/dead stained microglia in 3D collagen hydrogels

To quantify cell viability in each condition following extract exposure the confocal z-stack images of calcein-AM/EthD stained microglia were analysed using the Fiji version of the image analysis software ImageJ.[40] A 2D representation of the calcein-AM/EthD stained image stacks was prepared using the maximum intensity projection function. A copy of this projection, combining the calcein-AM and EthD fluorescence signals into a single channel, was prepared and processed using the rolling ball background subtraction and despeckle functions. A signal threshold was set and applied to generate a binary image, and adjacent cells with overlapping signals were delineated using the watershed function. Particle analysis was

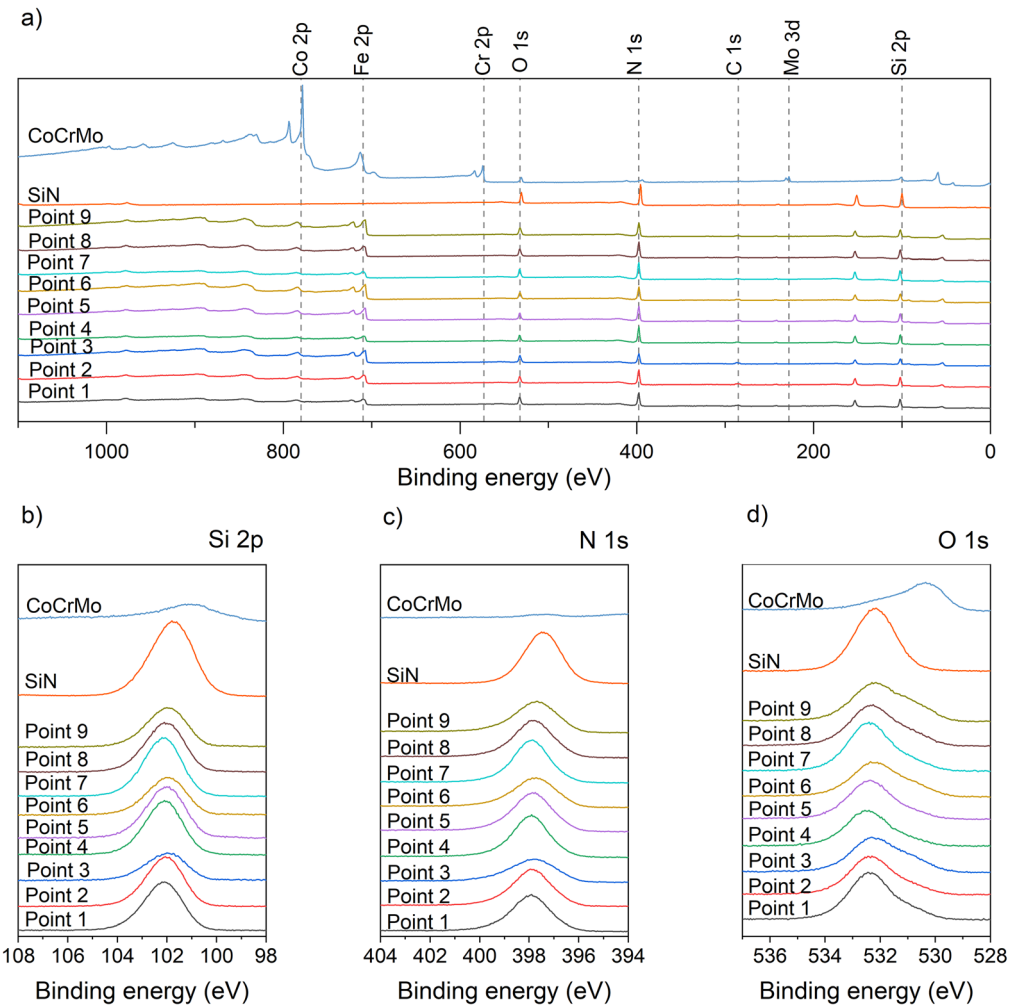

Fig. 3 XPS spectra of the native samples. A survey spectrum (a) reveals the expected peaks; Si, N, O, Fe and C for the coatings, Si, N and O for the SiN reference coating and Cr, Co and Mo for the CoCrMo reference. Elemental spectra for Si (b), N (c) and O (d) show similar behaviour for all the coatings.

applied to identify cells as individual regions of interest (ROI), which were recorded in the ROI manager. These ROIs were then overlaid on the separate calcein-AM and EthD channels and the mean fluorescence from each stain in each ROI was recorded. The relative calcein-AM and EthD fluorescence per cell was calculated as a percentage of the total cell fluorescence. An arbitrary live/dead inclusion cutoff was established based on analysis of the median calcein-AM signal (approx. 65% of total cell fluorescence) from cells treated 1 day with culture medium, and the median EthD signal (approx. 65% of total cell fluorescence) in cells treated 1 day with DMSO. The percentage of live cells for each condition's replicates were presented as scatterplots.

Statistical analysis

The statistical analysis was performed using IBM SPSS Statistics, version 28 (IBM Corp., Armonk, N.Y., USA). Cell studies were analyzed using a Kruskal–Wallis nonparametric test and differences between groups were determined with Dunn's–Bonferroni *post hoc* analysis. A p-value <0.05 was considered indicative of statistical significance.

Results

Material characterization

The composition of the SiFeCN coatings, determined using XPS, revealed expected gradients of Si ranging from 35.0 at% to 47.3 at%, Fe from 1.4 at% to 9.3 at% and C from 4.5 at% to 13.9 at% (Fig. 2). Notably, there was also a difference in N content (39.6 at% to 43.9 at%) despite N being supplied as a gas and hence the availability was expected to be the same regardless of position. In a similar manner there was a difference in O contaminations (2.1 at% to 5.1 at%).

A detailed examination of the XPS spectra for the deposited coatings (native) (Fig. 3) reveal the expected peaks. The survey spectra for the coatings all have peaks indicating the presence of Si, N, Fe, C and O, while the spectrum for the SiN reference

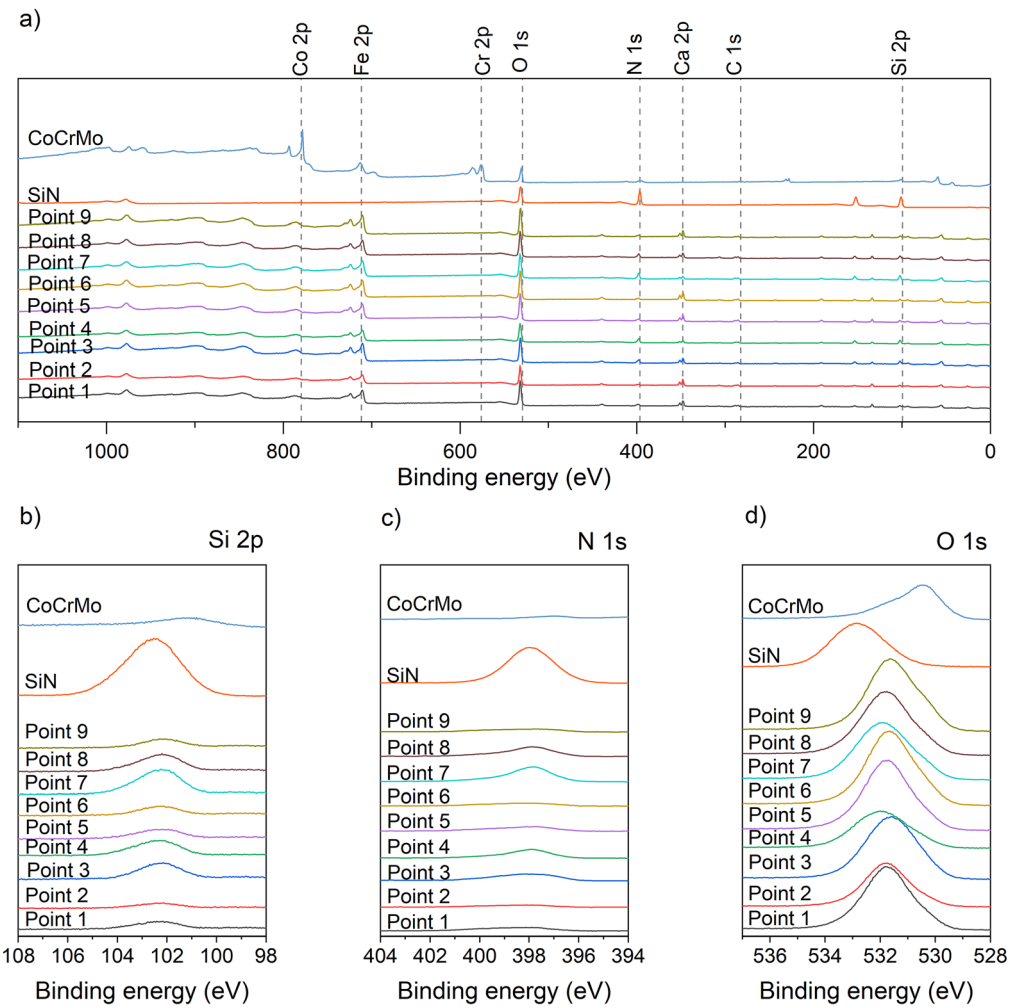

Fig. 4 XPS spectra of the exposed samples to cell media. The survey spectra (a) of the coatings now have a Ca peak in addition to the peaks attributed to the coating. The individual spectra (b–d) show less pronounced peaks for Si and N for the SiFeCN coatings and a shift of the O peak in the SiN coating (d) compared with the native sample.

has no Fe peak. The element spectra include a Si peak at 102 eV for the SiFeCN coatings, which is attributed to Si–N. Previous studies have found the Si–N contribution at 102.7 eV.[31] Further, the N peak was located at 398 eV, which is consistent with Si–N.[31] The O peak for the SiN samples is located at 532.2 eV, which is consistent with SiO_2.[41] The O peak for the SiFeCN coatings is wider and likely have several contributions, including Fe–O (530.5 eV (ref. 41)). Following dissolution in cell media the survey spectra for the exposed coatings exhibited a Ca contribution (Fig. 4). This was not observed in the SiN coating or the CoCrMo reference. Furthermore, there was a shift of the O peak for the SiN reference coating (from 532.2 eV to 532.85 eV) that was not observed for the SiFeCN coatings, which is probably due to a contribution of silanol groups (Si-OH) at 533.7 eV.[42]

After deposition the coating had a low surface roughness (Fig. 5: S_a ranging from 7.36 ± 0.95 nm to 11.08 ± 3.94 nm, S_q from 11.24 ± 3.07 nm to 15.29 ± 6.23 nm and S_z from 519 ± 171 nm to 948 ± 1063 nm) similar to the reference materials (CoCrMo with an S_a of 7.94 ± 1.10 nm, S_q of 10.97 ± 1.75 nm and S_z of 412 ± 194 nm and SiN with S_a of 7.97 ± 0.71 nm, S_q of 11.74 ± 3.27 nm and S_z of 613 ± 573 nm, Fig. 5).

Dissolution

Post dissolution the surface of the exposed coatings revealed evidence of increased porosity (Fig. 6). The surface of the CoCrMo reference exhibited little to no corrosion upon visual inspection. In contrast, the SiN reference coating revealed a profound change in surface appearance after just 14 days of dissolution. When examining the SiFeCN coating surfaces before (native) and after (exposed) dissolution, coatings with lower Si content (35.0 at%, 36.4 at% and 38.3 at%) revealed fewer changes to their surface appearance when compared to coatings with higher Si content (43.4 at%, 46.5 at% and 47.3 at%). The coatings with lower Si content had higher Fe or C content;

- point 3 (Si: 35.0 at%, Fe: 8.8 at%, C: 13.9 at%, N: 39.6 at% and O: 2.7 at%),
- point 6 (Si: 36.4 at%, Fe: 7.0 at%, C: 7.8 at%, N: 43.9 at% and O: 4.9 at%) and
- point 9 (Si: 38.3 at%, Fe: 9.3 at%, C: 5.7 at%, N: 41.8 at% and O: 4.9 at%)

compared with

- point 1 (Si: 43.44 at%, Fe: 1.86 at%, C: 8.15 at%, N: 43.53 at% and O: 3.01 at%),
- point 4 (Si: 46.46 at%, Fe: 2.01 at%, C: 6.85 at%, N: 40.93 at% and O: 3.74 at%) and
- point 7 (Si: 47.25 at%, Fe: 1.44 at%, C: 4.68 at%, N: 43.14 at% and O: 3.49 at%).

Cross-sections were used to determine thickness (Table 1) and morphology of the native and exposed coatings (Fig. 7). Three points, each with a different Si content (35.0 at% (point 3), 39.8 at% (point 5) and 47.3 at% (point 7)), and the reference SiN coating and CoCrMo controls were analysed. The thinnest native sample was point 3 (427 nm) and the thickest was point 7 (524 nm). The thickness of all three SiFeCN coatings was greater than the SiN coating reference, which had a thickness of 333 nm. Following exposure, the thinnest sample was again point 3 (353 nm) and the thickest was again point 7 (434 nm), and the SiN coating reference was 216 nm thick. The cross-section of point 7 (highest Si content) showed more pores than point 3 (lowest Si content). The CoCrMo revealed only a slight indication of dissolution while the SiN coating reference revealed more irregularities, which were partially filled with the platinum layer and exhibited more pores than the SiFeCN coatings.

The dissolution rate was estimated based on the reduction in thickness of the coating after 14 days in cell culture media. The SiN coating reference thickness was reduced by 117 nm, while the SiFeCN coatings were reduced by 73–95 nm. Therefore, the dissolution rates of 5.2–6.8 nm per day calculated for the SiFeCN coatings were lower than the 8.3 nm per day calculated for the SiN coating reference (Table 1).

The ion release measured in the extracts after 14 days exposure had lower levels of Si from the SiFeCN coatings than from the SiN reference (but higher than the CoCrMo reference) (Fig. 8), in agreement with the FIB results. The detected levels of Fe were higher in extracts from the SiFeCN coatings compared to both references (CoCrMo and SiN coating), as expected, and the levels of detected Co ions were reduced in extracts from the SiFeCN coatings and SiN reference coating compared to the CoCrMo reference. The latter indicates a general ability of the coatings to reduce the levels of metal ion release from the underlying substrate, while the ICP results revealed no significant difference in degree of ion release between the different compositions of the SiFeCN coatings (Fig. 8).

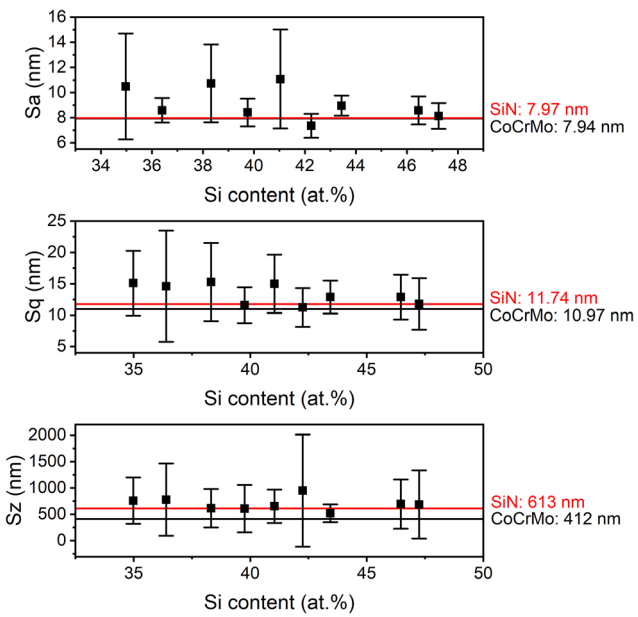

Fig. 5 Surface roughness parameters for coatings with varying Si content (mean ± standard deviation). The roughness of the references (CoCrMo and SiN) are depicted as lines.

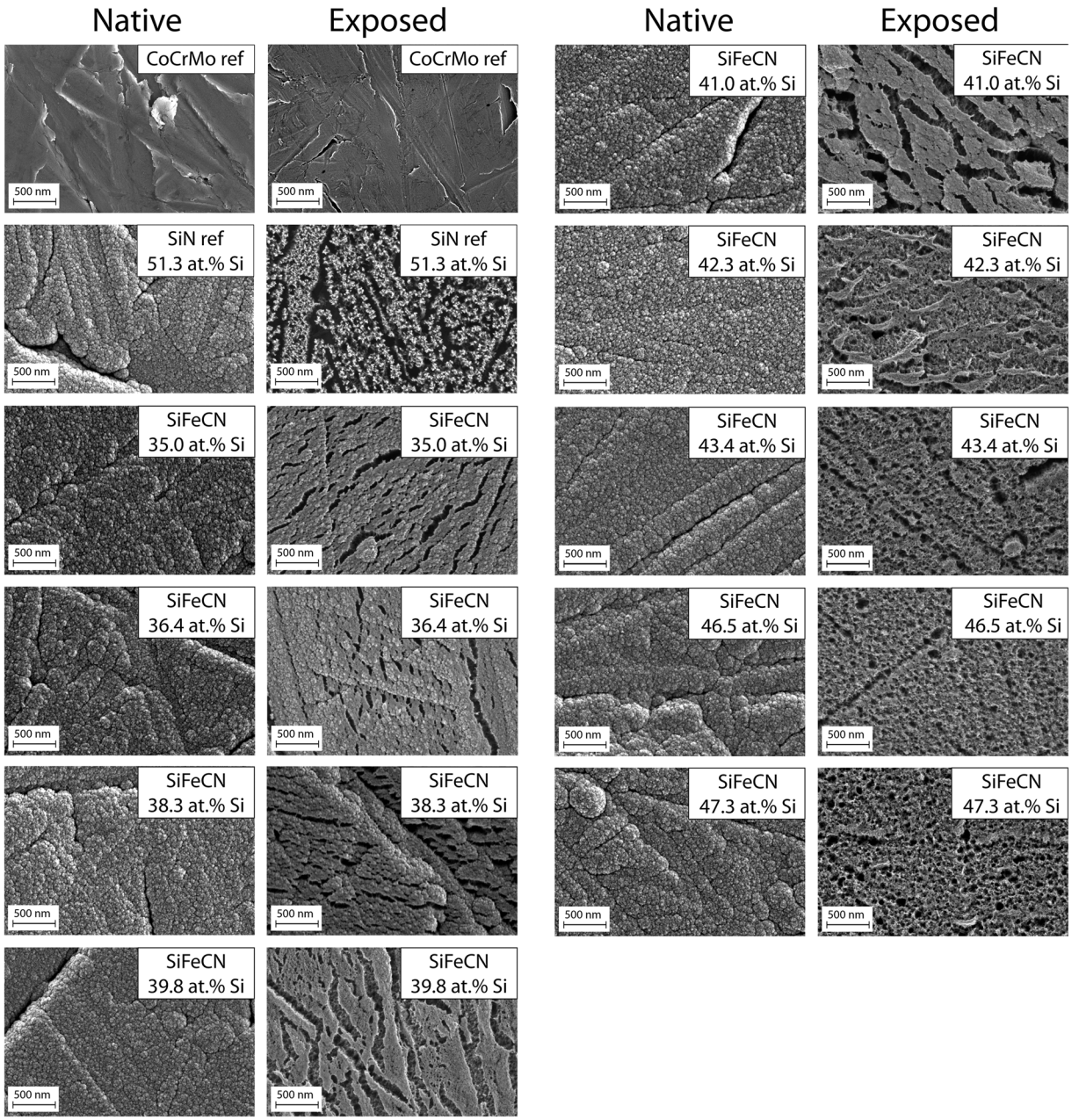

Fig. 6 SEM images of native and exposed CoCrMo (CoCrMo ref) and SiN coating (SiN ref) references, followed by SiFeCN coatings arranged in order of increasing Si content (35.0–47.3 at%).

Table 1 Chemical composition, thickness, thickness reduction and dissolution rate obtained from the FIB cross-sections

Point/ sample	Si (at%)	Fe (at%)	C (at%)	N (at%)	O (at%)	N/ Si	Native thickness (nm)	Thickness reduction (nm)	Dissolution rate (nm per day)
3	35.0	8.8	13.9	39.6	2.7	1.13	427	73	5.2
5	39.8	5.2	7.2	43.0	4.9	1.08	477	95	6.8
7	47.3	1.4	4.7	43.1	3.5	0.91	524	90	6.4
SiN ref.	51.3	—	1.0	36.7	11.0	0.72	333	117	8.3

Indirect cytotoxicity tests

A preliminary cytotoxicity study was conducted using microglia exposed to a dilution series (1 : 1, 1 : 8, 1 : 16, 1 : 32, 1 : 48, 1 : 64 and 1 : 80 dilution) of extracts from the SiN coating and CoCrMo reference controls, and two points of the SiFeCN coatings. Since CoCrMo and SiN are established biocompatible materials, their extracts were used to define the necessary

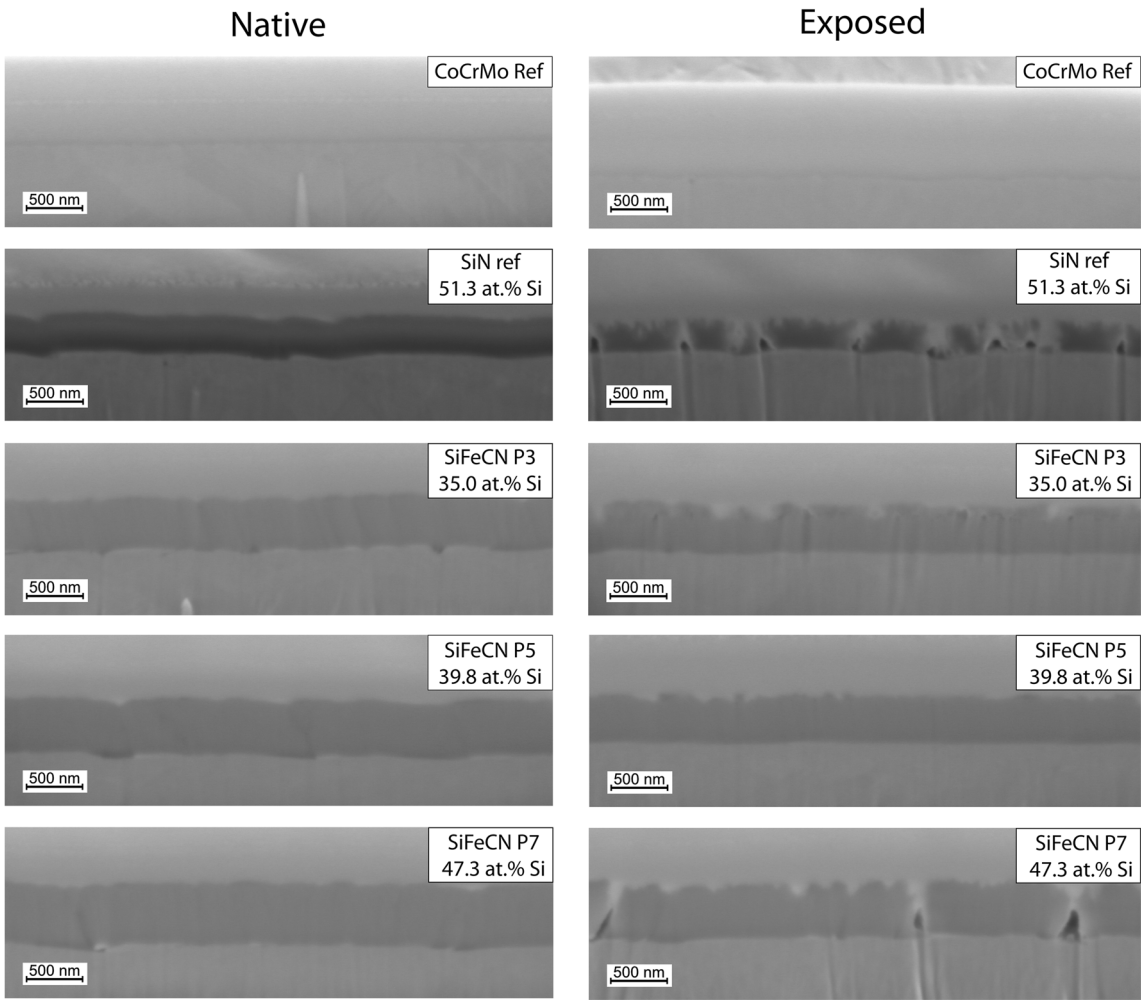

Fig. 7 SEM images of cross-sections of native and exposed SiFeCN coatings and CoCrMo and SiN coating references. The images are arranged the reference materials, CoCrMo and the SiN coating, in the top followed by the SiFeCN coatings with the lowest Si content (35.0 at%) to highest Si content (47.3 at%) with the point number indicated for each sample.

levels of dilution to assess the compatibility of the SiFeCN coatings. The 1 : 64 dilution was chosen to compare all the samples as it maintained sufficient cell viability to permit analysis of differences between the different extracts (see ESI, Fig. S1†). The cytotoxicity of the coatings was evaluated by exposing microglia for 1–3 days to cell media that had been in contact with the coatings for 14 days. Fig. 9 shows the cell viability in the presence of a 1 : 64 dilution of the different SiFeCN coating extracts at 1 : 64 dilution, where extracts from a SiN coating and an uncoated CoCrMo substrate were used as references. On day 1 (Fig. 9a) all the cultures including the ones treated with extracts from CoCrMo and SiN coating control showed mean viability levels above 80% of the untreated controls. On day 2 (Fig. 9b) there was a slight reduction in viability in all treatment conditions, which was statistically significant for three of the SiFeCN extracts, but all conditions yielded a mean viability of at least 70% compared to untreated controls. By day 3 (Fig. 9c) viability in cultures treated with the SiFeCN coating extracts were at a similar level to those seen at day 1 (81–96%), while those treated with extracts from the CoCrMo or SiN reference controls were significantly reduced (66%).

Microglial viability in 3D collagen hydrogels was assessed using live/dead staining. The hydrogels were imaged by confocal microscopy and the percentage of live cells was determined by image analysis and compared between conditions (details in materials and methods). Confocal *z*-stacks confirmed an even cell distribution throughout the hydrogels, and the untreated and DMSO-treated controls were readily distinguished by the calcein-AM (live) and EthD (dead) staining (Fig. 10a and b). Confocal images of the cultures treated with the different extracts presented with comparable levels of calcein-AM and EthD staining as observed in the untreated control (see ESI, Fig. S2†). On day 1 all the cultures exposed to the different extracts had an average cell viability above 70% (Fig. 10c), but only the extract from the CoCrMo reference (95% viability) was significantly different ($p < 0.05$) than the DMSO control. By day 3 (Fig. 10d) all cultures exposed to the

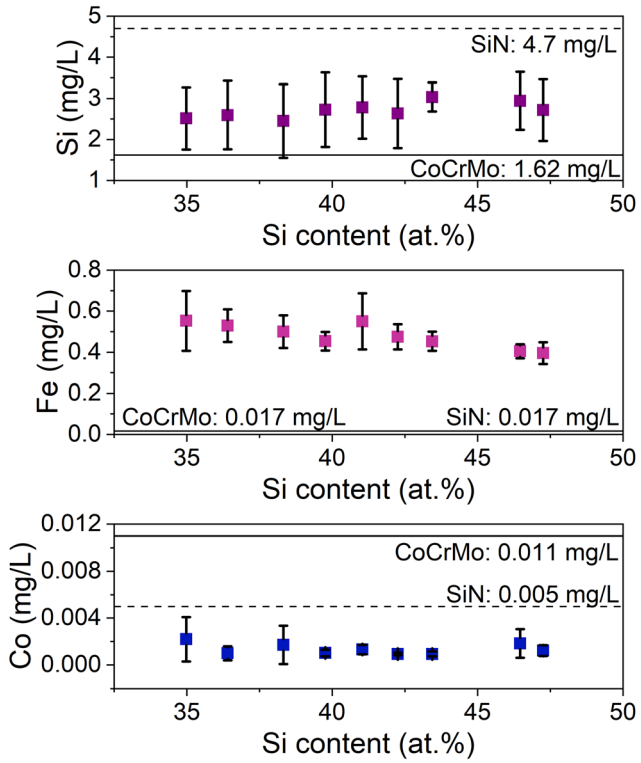

Fig. 8 Si, Fe and Co ion release of the coatings. The ions released from the CoCrMo and SiN coating reference materials are marked as solid and dashed lines, respectively.

coating extracts (including the SiN coating reference) had higher levels of viability (90–94%) than day 1, while cultures treated with the CoCrMo reference extract revealed a slight decrease in viability (92%) compared to day 1. There was no significant difference between the untreated control and any of the tested conditions. Only extracts from the control reference materials and the SiFeCN coating with Si content 39.8 at% revealed viability that was statistically significantly higher than the DMSO control, nonetheless all had mean viability levels above 80%.

Discussion

Identifying biocompatible coating compositions that reduce the release of metal ions and debris from metal implants will reduce the risk of various local and systemic adverse reactions to implants that have been observed in patients. In this study the effects of adding Fe and C to a SiN coating, which covered a CoCrMo substrate, was investigated. To efficiently evaluate different compositions, combinatorial sputtering was used to deposit coatings of compositional gradients onto the substrate surface. Nine individual CoCrMo discs were arranged in 3 × 3 grid prior to deposition. As CoCrMo is among the most common implant materials used in wearing surfaces,[43] it was selected here to evaluate the capacity of different coatings to reduce ion release from this underlying substrate. Implants composed of CoCr release Co ions, and systemic toxicity may occur if Co ions enter circulation, from where they can negatively impact *e.g.* the cardiovascular, respiratory, and nervous systems.[44] Local toxicity can also occur if Co ions are deposited in a specific tissue or organ, leading to damage and inflammation.[45] In addition, excessive exposure to Co ions can lead to the development of pseudotumors and has been linked to carcinogenicity.[46] Therefore, strategies that mitigate the release of Co ions from CoCrMo are of clinical significance. While the SiFeCN coatings investigated here have been developed previously,[36] their effectiveness in reducing ion release from an underlying substrate and their impact on coating dissolution rates had not been evaluated. In addition, as one of the intended applications would be to coat spinal implants, it was relevant to determine their compatibility with cells present in spinal tissues.

The range of the Si, Fe, and C gradients detected in the coatings were similar to what we have previously reported.[36] However, we did not observe a correlation between the N and Si content, which was previously attributed to Si bonding to N, which may be due to differences in other element contents present in the current study. C *e.g.* also has a certain affinity to Si.[47] The composition did not affect the surface roughness and the native surfaces of the SiFeCN coatings had a low surface roughness, with a cauliflower-like structure, which has previously been described.[36] An increase in the Si content of the coatings correlated with an increase in thickness, ranging from 427–524 nm, in accordance with our previous study.[36] Following dissolution, the surfaces of high Si content (and consequently low Fe content) coatings revealed a more uniform increase in surface porosity compared to those with low Si content, which appeared largely unchanged apart from a limited number of narrow open pores. The cross-section morphology supported these observations as more pores were apparent post-dissolution in higher Si content coatings, and a greater thickness reduction was observed in these coatings. Notably, we observed localized dissolution of primarily the SiN reference coating from the substrate (Fig. 7), which would presumably contribute to reduced implant functionality in a clinical context.[48]

We did not observe a correlation between the degree of Si content in the coatings and their release of Si ions. However, coatings containing Fe and C released less Si than the SiN coating reference, indicating their positive effect on the coatings' dissolution rate. This was further supported by the thickness reduction measurements, where the SiFeCN coatings revealed less reduction than the SiN reference. An increase in the N/Si ratio has previously been associated with a decreased dissolution rate,[49] and similarly here the higher dissolution rate of the SiN reference coating may in part be explained by its N/Si ratio (0.7), which was lower than the N/Si ratios of the SiFeCN coatings (>0.9). Additionally, the SiFeCN coating with the lowest dissolution rate (Fig. 7) also had lower O and higher Fe and C content, this may contribute to more Si–C bonds, which are more stable than Si–O bonds, and likely reduce the coatings reactivity. These data support previous findings where

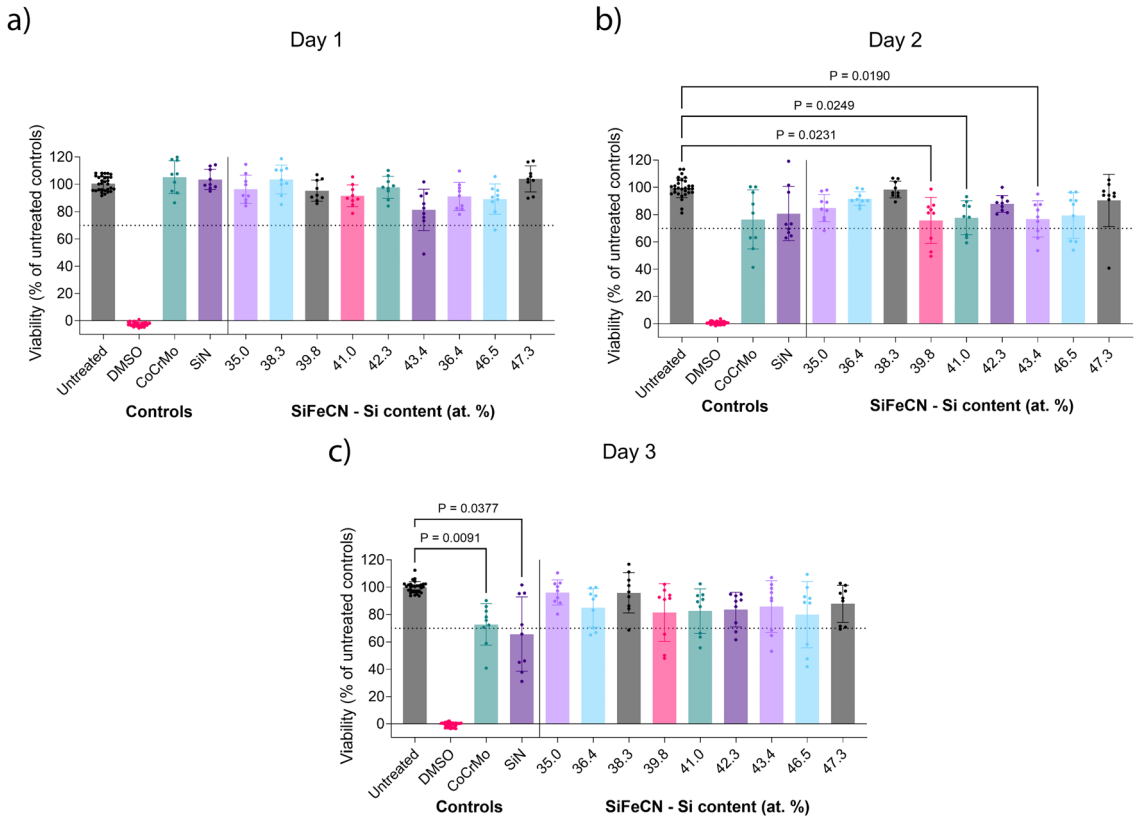

Fig. 9 Cell viability of C8-B4 cells in 2D culture in the presence of the different extracts at 1 : 64 dilution on day 1 (a), day 2 (b) and day 3 (c) (mean ± SD; n = 9). MTT assay was used to calculate cell viability. Statistically significant difference between samples (Kruskal–Wallis plus Dunn's–Bonferroni) is shown with the respective p-value. The threshold for cytotoxicity (70% viability of untreated control) is marked as a line in the graph.

Cr and Nb similarly reduced Si release from SiCrNbN coatings.[27] That data did however show a correlation of the ion release to the composition, namely the Cr content, which could be caused by the formation of a passivating oxide. The XPS elemental peaks also revealed a shift in the O peak for the exposed SiN coating, indicating a change in the bonding structure of the SiN coating that was not observed for the SiFeCN coatings (Fig. 4). This was most likely due to the faster dissolution rate of the more reactive SiN coating, giving raise to silanol groups on the surface. It has been reported that the reaction of SiN in aqueous solutions forms SiO_2 that can subsequently facilitate the formation of Si-OH groups.[50,51] Another interesting phenomenon was the detection of Ca post dissolution for the SiFeCN coatings. This was not observed for the CoCrMo or SiN coating reference, implying that the Ca present in the cell media only precipitated or reacted with the SiFeCN coatings. The implications of this reactivity in the context of materials intended for use as bone implants should be investigated further.

The duration of the extraction protocol (14 days) used to condition cell culture media for the indirect cytotoxicity tests was longer than that recommended in the ISO standard 10993,[39] this was due to the detection limit of the ICP-OES used to measure the ion release. Consequently, it was necessary to compensate for this with a high dilution of the extracts, the 1 : 64 dilution was chosen based on the viability levels obtained for CoCrMo and SiN reference controls over time. In a previous study, a similar extraction duration was used and required a 1 : 16 dilution of extracts before viability of fibroblasts was observed to be similar to untreated controls.[27] The microglia viability in 2D cultures exposed to a 1 : 64 dilution of extracts derived from the SiFeCN coatings was above 70% for all compositions tested. Any differences in viability between the samples proved not to be statistically significant, which may in part reflect that there were no significant differences between the degree of ion release from the SiFeCN coatings; however, there was also a high degree of variability between different experiments. There was a reduction in viability for the SiN reference coating compared to SiFeCN coatings, which may in part be explained by its higher dissolution rate, which has been previously observed for SiCrNbN coatings.[27] Other studies have found that Si ions can promote proliferation of cells, but an excessive Si concentration could be cytotoxic.[52]

Previous studies using adipose derived stem cells indicate that Fe extracts are cytocompatible,[53] but Fe is also an activator of microglia, enhancing the release of pro-inflammatory cytokines and playing an important role in several neurodegenerative pathologies *e.g.* Alzheimer's disease and Parkinson's disease.[54–56] Therefore, it was interesting to note that the Fe ion released from the SiFeCN coatings did not have a negative

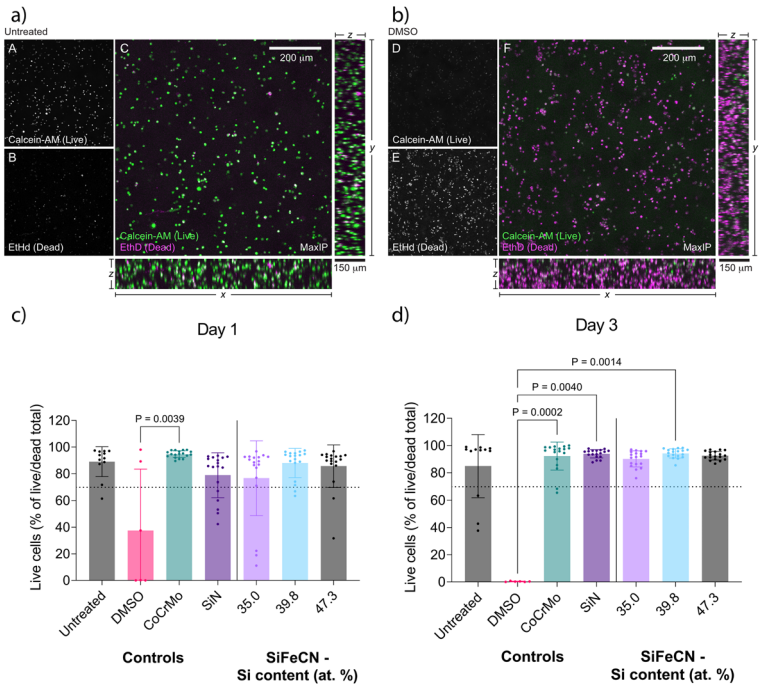

Fig. 10 Cell viability of C8-B4 cells in culture in 3D collagen hydrogels in the presence of the different extracts at 1 : 64 dilution over 3 days. Confocal laser scanning microscopy images at day 1 of untreated cells (a) and cell exposed to DMSO control (b). Green (calcein-AM) for living cells, magenta (EthD) for dead cells. The calculated percentage of live cells for day 1 (c) and 3 (d) (mean ± SD, each datapoint represents the % of live microglial cells in 1 of 3 images acquired from 1 of 6 collagen hydrogels treated for each condition (*i.e.* 18 datapoints/condition). Statistically significant difference between samples (Kruskal–Wallis plus Dunn's–Bonferroni) is shown with the respective *p*-value. The threshold for cytotoxicity (70% viability of untreated control) is marked as a line in the graph.

impact on microglia viability. CoCrMo extracts did adversely affect microglia viability, which could be attributed to high levels of Co ions, and this detrimental effect of CoCr wear particles and ions on glial viability has previously been reported.[57] Cobalt ions can exhibit cytotoxicity *in vitro* by interfering with intracellular processes and damage cell membranes, leading to cell death. This cytotoxicity has been observed in various cell types, including human cell lines and primary cells.[57,58] Nonetheless, since CoCrMo is an established material used in spinal implants, obtaining a comparable cell viability with the extracts from the SiFeCN coatings is considered a promising result, indicating that further evaluation of these materials is warranted.

Microglia viability in 3D collagen hydrogels was above 70% for all of the extracts tested, with no significant viability differences observed between the different extracts, which supports the results from the 2D cultures. In addition, there was no significant difference between any of the tested conditions with the untreated control in 3D. However, higher concentrations of DMSO were required to establish robust cell death in the 3D cultures compared to the experiments in 2D. Notably, in the 3D cultures CoCrMo extracts did not have an adverse effect on cell viability, which was in contrast to the decreased viability observed in 2D culture. A previous study reported no adverse effects on glial cells cultured with CoCr ions after 2 days; however, after 5 days viability decreased for one of the ion concentrations tested.[59] Further studies will be necessary to explore longer term effects of exposure to these coating extracts; however, in this study similar durations were maintained in the 2D and 3D experiments to facilitate comparisons between conditions, and after three days in 2D culture the microglia had reached confluence, limiting the possibility for comparisons at later time-points. Furthermore, in the 3D culture the cells showed an apparent increase in viability over time for almost all the tested conditions (*i.e.* there was a greater percentage of live cells at day 3 compared to day 1). In contrast, the opposite was observed for 2D culture with lower cell viability on day 3 compared to day 1 for almost all conditions tested. Several explanations for these apparent differences exist; for example, the relative surface area for cell growth is greater on the 3D collagen matrix than in 2D so the potential to observe proliferation is increased in the 3D setting. The presence of the collagen matrix may also provide support and adhesion sites that promote viability and reduce the cells sensitivity to certain insults. Furthermore, the collagen matrix may also interact with, or limit the diffusion of cytotoxic ions in the extracts, and in doing so reduce the cells' exposure to these. Microglia may also proliferate in response to pro-inflammatory stimuli so an increase in viability may reflect an activation state. Different effects for similar treatments have previously been reported between 2D and 3D cultures, and while 2D culture models may over-estimate adverse effects [37,59,60] they are a well-established, and relatively cost-effective model system, while 3D cultures permit the potential

influence of extracellular matrix models to be investigated. Finally, as both the MTT assay (used in the 2D culture) and the calcein-AM fluorescence (used in the 3D culture) report on viability as a product of metabolic and enzymatic (esterase) activity, any treatments that alter this cellular activity will also alter the apparent cell viability, so interpretations and direct comparisons should be cautiously considered.

While combinatorial investigations allow for efficient screening, they also come with challenges. The compositional gradients in this study extend in two directions (Fig. 1a), which means the investigated area should be limited, and not cover a range of compositions for each investigation. While areas of different sizes were investigated for different techniques, the composition of each sample was assumed to be uniform, which could be considered a limitation of the study; for example, ICP extracts were retrieved from an area of 50.3 mm^2, and the XPS used a spot size with a diameter of 100 μm. Thus, the composition will vary over the surface from which extracts for ICP are obtained and possible small differences in the investigated area will not be detected. This illustrates the possibility to efficiently screen a range of compositions, but also a need for further investigations. Future work should include tribocorrosive studies on homogenous coatings and long-term dissolution investigations. Further cell investigations will be necessary to assess potential genotoxic effects and to determine the inflammatory state of microglial cells exposed to coating extracts, which could in turn have paracrine effects on neighbouring astrocytes and neurons, which would likely be best evaluated in an *in vivo* study.

Conclusions

The aims of this study were to investigate the dissolution behaviour and cytotoxicity of SiFeCN coatings, in particular for potential future use in spinal applications. The incorporation of Fe and C into SiN coatings reduced the coatings' dissolution rate, and microglia cell viability in 2D and 3D cultures was similar for these SiFeCN coatings as for the clinically relevant CoCrMo reference material, and a SiN coating control. Further investigations are thus merited to explore the potential viability of SiFeCN coatings for future spinal implants.

Author contributions

Conceptualization, E. E., C. S., and C. P.; methodology, E. E., C. S., P. O. C., A. P., J. K., G. H.-B. and C. P.; investigation, E. E., C. S., A. P. and P. O. C.; formal analysis, E. E., C. S., P. O. C. and A. P.; data curation, E. E., C. S., and C. P.; writing – original draft preparation, E. E., and C. S.; writing – review and editing, P. O. C., A. P., J. K., G. H.-B. and C. P.; supervision, J. K., G. H.-B. and C. P.; funding acquisition, A. P., J. K. and C. P. All authors have read and agreed to the published version of the manuscript.

Conflicts of interest

The authors declare no conflict of interest.

Acknowledgements

Funding was received from the European Union's Seventh Framework Program (FP7/2007-2013), grant agreement GA-310477(Life-Long Joints), the European Union's Horizon 2020 research and innovation programme under the Marie Skłodowska-Curie grant agreement no. 812765 (NU-SPINE), Swedish Research Council (2020-04715), Cancerfonden, grant number 20 1285 PjF and Lennander's and Liljevalch's scholarships.

The authors would like to thank Pedro Berastegui for his assistance with certain depositions and XPS measurements.

References

1 D. J. Langton, T. J. Joyce, S. S. Jameson, J. Lord, M. Van Orsouw, J. P. Holland, A. V. F. Nargol and K. A. De Smet, Adverse Reaction to Metal Debris Following Hip Resurfacing: The Influence of Component Type, Orientation and Volumetric Wear, *J. Bone Jt. Surg. – Ser. B*, 2011, **93**, 164–171, DOI: **10.1302/0301-620X.93B2.25099**.

2 N. J. Hallab, A Review of the Biologic Effects of Spine Implant Debris: Fact from Fiction, *SAS J.*, 2009, **3**, 143–160, DOI: **10.1016/j.esas.2009.11.005**.

3 R. Ayers, M. Miller, J. Schowinsky, E. Burger, V. Patel and C. Kleck, Three Cases of Metallosis Associated with Spine Instrumentation, *J. Mater. Sci. Mater. Med.*, 2018, **29**, 3, DOI: **10.1007/s10856-017-6011-7**.

4 A. J. Mitchelson, C. J. Wilson, W. M. Mihalko, T. M. Grupp, B. T. Manning, D. A. Dennis, S. B. Goodman, T. H. Tzeng, S. Vasdev and K. J. Saleh, Biomaterial Hypersensitivity: Is It Real? Supportive Evidence and Approach Considerations for Metal Allergic Patients Following Total Knee Arthroplasty, *BioMed Res. Int.*, 2015, **2015**, 137287, DOI: **10.1155/2015/137287**.

5 E. Gibon, D. F. Amanatullah, F. Loi, J. Pajarinen, A. Nabeshima, Z. Yao, M. Hamadouche and S. B. Goodman, The Biological Response to Orthopaedic Implants for Joint Replacement: Part I: Metals, *J. Biomed. Mater. Res., Part B*, 2017, **105**, 2163–2173, DOI: **10.1002/jbm.b.33734.The**.

6 I. Papageorgiou, T. Abberton, M. Fuller, J. L. Tipper, J. Fisher and E. Ingham, Biological Effects of Clinically Relevant CoCr Nanoparticles in the Dura Mater: An Organ Culture Study, *Nanomaterials*, 2014, **4**, 485–504, DOI: **10.3390/nano4020485**.

7 I. Papageorgiou, R. Marsh, J. L. Tipper, R. M. Hall, J. Fisher and E. Ingham, Interaction of Micron and Nano-Sized Particles with Cells of the Dura Mater, *J. Biomed. Mater.*

Res., Part B, 2014, **102**, 1496–1505, DOI: 10.1002/jbm.b.33129.

8 B. Behl, I. Papageorgiou, C. Brown, R. Hall, J. L. Tipper, J. Fisher and E. Ingham, Biological Effects of Cobalt-Chromium Nanoparticles and Ions on Dural Fibroblasts and Dural Epithelial Cells, *Biomaterials*, 2013, **34**, 3547–3558, DOI: 10.1016/j.biomaterials.2013.01.023.

9 P. Korovessis, G. Petsinis, M. Repanti and T. Repantis, Metallosis After Contemporary Metal-on-Metal Total Hip Arthroplasty, *J. Bone Jt. Surg.*, 2006, **88**, 1183–1191, DOI: 10.2106/JBJS.D.02916.

10 S. Natu, R. P. Sidaginamale, J. Gandhi, D. J. Langton and A. V. F. Nargol, Adverse Reactions to Metal Debris: Histopathological Features of Periprosthetic Soft Tissue Reactions Seen in Association with Failed Metal on Metal Hip Arthroplasties, *J. Clin. Pathol.*, 2012, **65**, 409–418, DOI: 10.1136/jclinpath-2011-200398.

11 B. Braun, AS Advanced Surface – 7 Layers to Protect You Available online: https://www.bbraun.com/en/products/b0/as-advanced-surface.html%0A (accessed on 11 July 2018).

12 J. Reich, L. Hovy, H. L. Lindenmaier, R. Zeller, J. Schwiesau, P. Thomas and T. M. Grupp, Präklinische Ergebnisse Beschichteter Knieimplantate Für Allergiker, *Orthopade*, 2010, **39**, 495–502, DOI: 10.1007/s00132-009-1581-9.

13 J. K. Hofer and K. A. Ezzet, The Knee A Minimum 5-Year Follow-up of an Oxidized Zirconium Femoral Prosthesis Used for Total Knee Arthroplasty, *Knee*, 2014, **21**, 168–171, DOI: 10.1016/j.knee.2013.08.015.

14 M. Innocenti, R. Civinini, C. Carulli, F. Matassi and M. Villano, The 5-year results of an oxidized zirconium femoral component for TKA, *Clin. Orthop. Relat. Res.*, 2010, **468**(5), 1258–1263, DOI: 10.1007/s11999-009-1109-y.

15 F. Boschetto, N. Toyama, S. Horiguchi and R. M. Bock, In Vitro Antibacterial Activity of Oxide and Non-Oxide Bioceramics for Arthroplastic Devices: II. Fourier Transform Infrared Spectroscopy, *Analyst*, 2018, 2128–2140, DOI: 10.1039/c8an00234g.

16 M. Ishikawa, K. L. D. M. Bentley, B. J. Mcentire, E. M. Schwarz, C. Xie and B. S. Bal, Surface Topography of Silicon Nitride Affects Antimicrobial and Osseointegrative Properties of Tibial Implants in a Murine Model, *J. Biomed. Mater. Res., Part A*, 2017, 3413–3421, DOI: 10.1002/jbm.a.36189.

17 G. Pezzotti, R. M. Bock, B. J. McEntire, T. Adachi, E. Marin, F. Boschetto, W. Zhu, O. Mazdad and S. B. Bal, In Vitro Antibacterial Activity of Oxide and Non- Oxide Bioceramics for Arthroplastic Devices: I. In Situ Time-Lapse Raman Spectroscopy, *R. Soc. Chem.*, 2018, **143**, 3708–3721, DOI: 10.1039/c8an00233a.

18 G. Pezzotti, R. M. Bock, B. J. Mcentire, E. Jones, M. Bo, W. Zhu, G. Baggio, F. Boschetto, L. Puppulin, T. Adachi, *et al.*, Silicon Nitride Bioceramics Induce Chemically Driven Lysis in Porphyromonas Gingivalis, *Langmuir*, 2016, **32**, 3024–3035, DOI: 10.1021/acs.langmuir.6b00393.

19 C. Skjöldebrand, S. Schmidt, V. Vuong, M. Pettersson, K. Grandfield, H. Högberg, H. Engqvist and C. Persson, Influence of Substrate Heating and Nitrogen Flow on the Composition, Morphological and Mechanical Properties of SiNx Coatings Aimed for Joint Replacements, *Materials*, 2017, **10**, 1–11, DOI: 10.3390/ma10020173.

20 M. Pettersson, C. Skjöldebrand, L. Filho, H. Engqvist and C. Persson, Morphology and Dissolution Rate of Wear Debris from Silicon Nitride Coatings, *ACS Biomater. Sci. Eng.*, 2016, **2**, 998–1004, DOI: 10.1021/acsbiomaterials.6b00133.

21 M. Pettersson, T. Berlind, S. Schmidt, S. Jacobson, L. Hultman, C. Persson and H. Engqvist, Structure and Composition of Silicon Nitride and Silicon Carbon Nitride Coatings for Joint Replacements, *Surf. Coat. Technol.*, 2013, **235**, 827–834, DOI: 10.1016/j.surfcoat.2013.09.008.

22 J. Olofsson, M. Pettersson, N. Teuscher, A. Heilmann, K. Larsson, K. Grandfield, C. Persson, S. Jacobson and H. Engqvist, Fabrication and Evaluation of SixNy Coatings for Total Joint Replacements, *J. Mater. Sci. Mater. Med.*, 2012, **23**, 1879–1889, DOI: 10.1007/s10856-012-4625-3.

23 T. Hänninen, S. Schmidt, I. G. Ivanov, J. Jensen, L. Hultman and H. Högberg, Surface & Coatings Technology Silicon Carbonitride Thin Films Deposited by Reactive High Power Impulse Magnetron Sputtering, *Surf. Coat. Technol.*, 2018, **335**, 248–256, DOI: 10.1016/j.surfcoat.2017.12.037.

24 S. Schmidt, T. Hänninen, J. Wissting, L. Hultman, N. Goebbels, A. Santana, M. Tobler and H. Högberg, SiNx Coatings Deposited by Reactive High Power Impulse Magnetron Sputtering: Process Parameters Influencing the Residual Coating Stress, *J. Appl. Phys.*, 2017, **121**, 171904, DOI: 10.1063/1.4977812.

25 M. Pettersson, S. Tkachenko, S. Schmidt, T. Berlind, S. Jacobson, L. Hultman, H. Engqvist and C. Persson, Mechanical and Tribological Behavior of Silicon Nitride and Silicon Carbon Nitride Coatings for Total Joint Replacements, *J. Mech. Behav. Biomed. Mater.*, 2013, **25**, 41–47, DOI: 10.1016/j.jmbbm.2013.05.002.

26 S. Lal, E. A. Caseley, R. M. Hall and J. L. Tipper, Biological Impact of Silicon Nitride for Orthopaedic Applications: Role of Particle Size, Surface Composition and Donor Variation, *Sci. Rep.*, 2018, **8**, 1–12, DOI: 10.1038/s41598-018-27494-y.

27 C. Skjöldebrand, E. Echeverri, G. Hulsart-Billström and C. Persson, Tailoring the Dissolution Rate and in Vitro Cell Response of Silicon Nitride Coatings through Combinatorial Sputtering with Chromium and Niobium, *Biomater. Sci.*, 2022, **10**, 3757–3769, DOI: 10.1039/d1bm01978c.

28 Y. Li, C. Wong, J. Xiong, P. Hodgson and C. Wen, Cytotoxicity of Titanium and Titanium Alloying Elements, *J. Dent. Res.*, 2010, **89**, 493–497, DOI: 10.1177/0022034510363675.

29 T. Berlind, N. Hellgren, M. P. Johansson and L. Hultman, Microstructure, Mechanical Properties, and Wetting Behavior of Si–C–N Thin Films Grown by Reactive Magnetron Sputtering, *Surf. Coat. Technol.*, 2001, **141**, 145–155, DOI: 10.1016/S0257-8972(01)01236-1.

30 T. Thärigen, G. Lippold, V. Riede, M. Lorenz, K. J. Koivusaari, D. Lorenz, S. Mosch, P. Grau, R. Hesse, P. Streubel, *et al.*, Hard Amorphous CSixNy Thin Films Deposited by RF Nitrogen Plasma Assisted Pulsed Laser Ablation of Mixed Graphite/Si3N4-Targets, *Thin Solid Films*, 1999, **348**, 103–113, DOI: **10.1016/S0040-6090(99)00024-3**.

31 C. W. Chen, C. C. Huang, Y. Y. Lin, L. C. Chen and K. H. Chen, The Affinity of Si-N and Si-C Bonding in Amorphous Silicon Carbon Nitride (a-SiCN) Thin Film, *Diamond Relat. Mater.*, 2005, **14**, 1126–1130, DOI: **10.1016/j.diamond.2004.10.045**.

32 T. Huang, J. Cheng and Y. F. Zheng, In Vitro Degradation and Biocompatibility of Fe – Pd and Fe – Pt Composites Fabricated by Spark Plasma Sintering, *Mater. Sci. Eng., C*, 2014, **35**, 43–53, DOI: **10.1016/j.msec.2013.10.023**.

33 M. Peuster, C. Hesse, T. Schloo, C. Fink, P. Beerbaum and C. von Schnakenburg, Long-Term Biocompatibility of a Corrodible Peripheral Iron Stent in the Porcine Descending Aorta, *Biomaterials*, 2006, **27**, 4955–4962, DOI: **10.1016/j.biomaterials.2006.05.029**.

34 R. Waksman, R. Pakala, R. Baffour, R. Seabron, D. Hellinga and F. O. Tio, Short-Term Effects of Biocorrodible Iron Stents in Porcine Coronary Arteries, *J. Interv. Cardiol.*, 2008, **21**, 15–20, DOI: **10.1111/j.1540-8183.2007.00319.x**.

35 M. Peuster, P. Wohlsein, M. Brügmann, M. Ehlerding, K. Seidler, C. Fink, H. Brauer, A. Fischer and G. Hausdorf, A Novel Approach to Temporary Stenting: Degradable Cardiovascular Stents Produced from Corrodible Metal - Results 6–18 Months after Implantation into New Zealand White Rabbits, *Heart*, 2001, **86**, 563–569, DOI: **10.1136/heart.86.5.563**.

36 C. Skjöldebrand, G. Hulsart-Billström, H. Engqvist and C. Persson, Si-Fe-C-N Coatings for Biomedical Applications: A Combinatorial Approach, *Materials*, 2020, **13**, 1–16, DOI: **10.3390/ma13092074**.

37 R. T. Y. Haw, C. K. Tong, A. Yew, H. C. Lee, J. B. Phillips and S. Vidyadaran, A Three-Dimensional Collagen Construct to Model Lipopolysaccharide-Induced Activation of BV2 Microglia, *J. Neuroinflammation*, 2014, **11**, 1–10, DOI: **10.1186/1742-2094-11-134**.

38 A. Frisk, F. Magnus, S. George, U. B. Arnalds and G. Andersson, Tailoring Anisotropy and Domain Structure in Amorphous TbCo Thin Films through Combinatorial Methods, *J. Phys. D: Appl. Phys.*, 2016, **49**, 035005, DOI: **10.1088/0022-3727/49/3/035005**.

39 Standardization, I.O., for ISO 10993-5 Biological Evaluation of Medical Devices. 61010-1 *© Iec:2001*, **2006**, *2006*, 13.

40 C. A. Schneider, W. S. Rasband and K. W. Eliceiri, NIH Image to ImageJ: 25 Years of Image Analysis, *Nat. Methods*, 2012, **9**, 671–675, DOI: **10.1038/nmeth.2089**.

41 N. R. Murphy, C. V. Ramana, L. Sun, J. G. Jones and J. T. Grant, Reactive Co-Sputtering of Hematite Doped Silica (Fe 2 O 3 -SiO 2) Thin Fi Lms, *J. Alloys Compd.*, 2017, **708**, 947–954, DOI: **10.1016/j.jallcom.2017.03.050**.

42 P. Post, L. Wurlitzer, W. Maus-Friedrichs and A. P. Weber, Characterization and Applications of Nanoparticles Modified In-Flight with Silica or Silica-Organic Coatings, *Nanomaterials*, 2018, **8**, 1–19, DOI: **10.3390/nano8070530**.

43 ISO 5832-4:2014 *Implants for Surgery - Metallic Materials - Part 4: Cobalt-Chromium-Molybdenum Casting Alloy*, 2014.

44 L. Leyssens, B. Vinck, C. van der Straeten, F. Wuyts and L. Maes, Cobalt Toxicity in Humans—A Review of the Potential Sources and Systemic Health Effects, *Toxicology*, 2017, **387**, 43–56, DOI: **10.1016/j.tox.2017.05.015**.

45 J. R. Campbell and M. P. Estey, Metal Release from Hip Prostheses: Cobalt and Chromium Toxicity and the Role of the Clinical Laboratory, *Clin. Chem. Lab. Med.*, 2013, **51**, 213–220, DOI: **10.1515/cclm-2012-0492**.

46 A. C. Cheung, S. Banerjee, J. J. Cherian, F. Wong, J. Butany, C. Gilbert, C. Overgaard, K. Syed, M. G. Zywiel, J. J. Jacobs, *et al.*, Systemic Cobalt Toxicity from Total Hip Arthroplasties, *Bone Jt. J.*, 2016, **98B**, 6–13, DOI: **10.1302/0301-620X.98B1.36374**.

47 T. Berlind, N. Hellgren, M. P. Johansson and L. Hultman, *Microstructure, Mechanical Properties, and Wetting Behavior of SiCN Thin Films Grown by Reactive Magnetron Sputtering*, 2001, vol. 141.

48 C. Skjöldebrand, J. L. Tipper, P. Hatto, M. Bryant, R. M. Hall and C. Persson, Current Status and Future Potential of Wear-Resistant Coatings and Articulating Surfaces for Hip and Knee Implants, *Mater. Today Bio*, 2022, **15**, 100270, DOI: **10.1016/j.mtbio.2022.100270**.

49 M. Pettersson, M. Bryant, S. Schmidt, H. Engqvist, R. M. Hall, A. Neville and C. Persson, Dissolution Behaviour of Silicon Nitride Coatings for Joint Replacements, *Mater. Sci. Eng., C*, 2016, **62**, 497–505, DOI: **10.1016/j.msec.2016.01.049**.

50 I. Katsaros, Y. Zhou, K. Welch, W. Xia, C. Persson and H. Engqvist, Bioactive Silicon Nitride Implant Surfaces with Maintained Antibacterial Properties, *J. Funct. Biomater.*, 2022, **13**(3), 129, DOI: **10.3390/jfb13030129**.

51 X. Du, S. S. Lee, G. Blugan and S. J. Ferguson, Silicon Nitride as a Biomedical Material: An Overview, *Int. J. Mol. Sci.*, 2022, **23**, 6551, DOI: **10.3390/ijms23126551**.

52 M. Y. Shie, S. J. Ding and H. C. Chang, The Role of Silicon in Osteoblast-like Cell Proliferation and Apoptosis, *Acta Biomater.*, 2011, **7**, 2604–2614, DOI: **10.1016/j.actbio.2011.02.023**.

53 T. C. Paim, D. P. Wermuth, I. Bertaco, C. Zanatelli, L. I. S. Naasani, M. Slaviero, D. Driemeier, L. Schaeffer and M. R. Wink, Evaluation of in Vitro and in Vivo Biocompatibility of Iron Produced by Powder Metallurgy, *Mater. Sci. Eng., C*, 2020, **115**, 111129, DOI: **10.1016/j.msec.2020.111129**.

54 D. W. Donley, M. Realing, J. P. Gigley and J. H. Fox, Iron Activates Microglia and Directly Stimulates Indoleamine-2,3-Dioxygenase Activity in the N171-82Q Mouse Model of Huntington's Disease, *PLoS One*, 2021, **16**, e0250606, DOI: **10.1371/journal.pone.0250606**.

55 B. Kenkhuis, A. Somarakis, L. de Haan, O. Dzyubachyk, M. E. Ijsselsteijn, N. F. C. C. de Miranda, B. P. F. Lelieveldt, J. Dijkstra, W. M. C. van Roon-Mom, T. Höllt, *et al.*, Iron

Loading Is a Prominent Feature of Activated Microglia in Alzheimer's Disease Patients, *Acta Neuropathol. Commun.*, 2021, **9**, 27, DOI: **10.1186/s40478-021-01126-5**.

56 R. C. McCarthy, J. C. Sosa, A. M. Gardeck, A. S. Baez, C. H. Lee and M. Wessling-Resnick, Inflammation-Induced Iron Transport and Metabolism by Brain Microglia, *J. Biol. Chem.*, 2018, **293**, 7853–7863, DOI: **10.1074/jbc.RA118.001949**.

57 L. J. Smith, A. L. Holmes, S. K. Kandpal, M. D. Mason, T. Zheng and J. P. Wise, The Cytotoxicity and Genotoxicity of Soluble and Particulate Cobalt in Human Lung Fibroblast Cells, *Toxicol. Appl. Pharmacol.*, 2014, **278**, 259–265, DOI: **10.1016/j.taap.2014.05.002**.

58 T. Laumonier, E. Ruffieux, J. Paccaud, V. Kindler and D. Hannouche, In Vitro Evaluation of Human Myoblast Function after Exposure to Cobalt and Chromium Ions, *J. Orthop. Res.*, 2020, **38**, 1398–1406, DOI: **10.1002/jor.24579**.

59 H. Lee, J. B. Phillips, R. M. Hall and J. L. Tipper, Neural Cell Responses to Wear Debris from Metal-on-Metal Total Disc Replacements, *Eur. Spine J.*, 2020, **29**, 2701–2712, DOI: **10.1007/s00586-019-06177-w**.

60 Y. Bédouin, P. Pellen Mussi, S. Tricot-Doleux, D. Chauvel-Lebret, P. Auroy, X. Ravalec, H. Oudadesse and F. Pérez, 3D Cell Culture to Determine in Vitro Biocompatibility of Bioactive Glass in Association with Chitosan, *Biomed. Mater. Eng.*, 2015, **26**, 169–181, DOI: **10.3233/BME-151555**.